J|A|C|S
ARTICLES
Published on Web 01/17/2007

Structures of Alkali Metals in Silica Gel Nanopores: New Materials for Chemical Reductions and Hydrogen Production

Mouath Shatnawi,[†] Gianluca Paglia,[†] James L. Dye,*[,‡,§] Kevin C. Cram,[‡] Michael Lefenfeld,*[,§] and Simon J. L. Billinge*[,†]

Contribution from the Department of Physics and Astronomy, Michigan State University, Biomedical and Physical Sciences Building, East Lansing, Michigan 48824-2320, Department of Chemistry, Michigan State University, East Lansing, Michigan 48824-2320, and SiGNa Chemistry, LLC, 530 East 76th Street, Suite 9E, New York, New York 10021

Received October 5, 2006; E-mail: billinge@pa.msu.edu; dye@msu.edu; michael@signachem.com

Abstract: Alkali metals and their alloys can be protected from spontaneous reaction with dry air by intercalation (with subsequent heating) into the pores of silica gel (SG) at loadings up to 40 wt %. The resulting loose, black powders are convenient materials for chemical reduction of organic compounds and the production of clean hydrogen. The problem addressed in this paper is the nature of the reducing species present in these amorphous materials. The atomic pair distribution function (PDF), which considers both Bragg and diffuse scattering components, was used to examine their structures. Liquid Na−K alloys added to silica gel at room temperature (stage 0) or heated to 150 °C (stage I) as well as stage I Na−SG, retain the overall pattern of pure silica gel. Broad oscillations in the PDF show that added alkali metals remain in the pores as nanoscale metal clusters. ^{23}Na MAS NMR studies confirm the presence of Na^0 and demonstrate that Na^+ ions are formed as well. The relative amounts of Na^0 and Na^+ depend on both the overall metal loading and the average pore size. The results suggest that ionization occurs near or in the SiO_2 walls, with neutral metal present in the larger cavities. The fate of the electrons released by ionization is uncertain, but they may add to the silica gel lattice, or form an "electride-like plasma" near the silica gel walls. A remaining mystery is why the stage I material does not show a melting endotherm of the encapsulated metal and does not react with dry oxygen. Na−SG when heated to 400 °C (stage II) yields a dual-phase reaction product that consists of Na_4Si_4 and Na_2SiO_3.

Introduction

Alkali metals are powerful reducing agents that are often used free or in solution in liquid ammonia to reduce organic compounds. However, because they react spontaneously with air, their use on a large scale is a continuing concern for synthetic and industrial chemists. A variety of adducts of alkali metals to inert supports have been developed to provide alternate reducing materials.[1−4] Recently, new materials with essentially the same reducing power as the parent alkali metals were developed by intercalation of up to 40 wt % of liquid alkali metals into the nanopores of amorphous silica gel.[5] These materials are nonpyrophoric and have good stability in dry air, making them easy to handle and easing storage concerns. These aspects of the alkali metal silica gel (M−SG) materials make them ideal candidates as reactants for large-scale hydrogen production and reduction chemistry. Despite their promise, the precise nature of the intercalated metals was not known.[5] We report here the use of the atomic pair distribution function (PDF) method[6,7] to determine their structures, supplemented by ^{23}Na MAS NMR studies. Alkali metals near the silica gel walls ionize, probably to yield M^+ and e^-, similar to zeolite-based "inorganic electrides".[8−10] When these sites are saturated, alkali metal nanocrystals form in the larger pores of the silica gel. After processing at higher temperature to get stage II material, the alkali metal is shown to react with the silica host, resulting in nanocrystalline Na_4Si_4 and Na_2SiO_3 products.

As previously reported,[5] the various silica gel samples used to prepare M−SG were calcined at 600 °C before use and consisted of irregularly shaped powders of size 0.25−0.7 mm with average pore diameters of 30, 60, and 150 Å. The resulting loose powders can contain as much as 60 mol % alkali metal and, with suitable heat treatment, do not react rapidly with dry

[†] Department of Physics and Astronomy, Michigan State University.
[‡] Department of Chemistry, Michigan State University.
[§] SiGNa Chemistry, LLC.

(1) Levy, J.; Tamarkin, D.; Selig, H.; Rabinovitz, M. *Angew. Chem., Int. Ed. Engl.* **1981**, *20*, 1033.
(2) Savoia, D.; Trombini, C.; Umani-Ronchi, A. *Pure Appl. Chem.* **1985**, *57*, 1887−1896.
(3) Birch, A. J. *Pure Appl. Chem.* **1999**, *68*, 553−556.
(4) Furstner, A.; Seidel, G. *Synthesis* **1995**, 63−68.
(5) Dye, J. L.; Cram, K. D.; Urbin, S. A.; Redko, M. Y.; Jackson, J. E.; Lefenfeld, M. *J. Am. Chem. Soc.* **2005**, *127*, 9338−9339.
(6) Peterson, P. F.; Proffen, T.; Jeong, I.-K.; Billinge, S. J. L.; Choi, K.-S.; Kanatzidis, M. G.; Radaelli, P. G. *Phys. Rev. B* **2001**, *63*, 165211.
(7) Egami, T.; Billinge, S. J. L. *Underneath the Bragg Peaks: Structural Analysis of Complex Materials*; Pergamon Press: Elsevier: Oxford, England, 2003; pp 55−98.
(8) Ichimura, A. S.; Dye, J. L.; Camblor, M. A.; Villaescusa, L. A. *J. Am. Chem. Soc.* **2002**, *124*, 1170−1171.
(9) Wernette, D. P.; Ichimura, A. S.; Urbin, S. A.; Dye, J. L. *Chem. Mater.* **2003**, *15*, 1441−1448.
(10) Petkov, V.; Billinge, S. I.; Vogt, T.; Ichimura, A. S.; Dye, J. L. *Phys. Rev. Lett.* **2002**, *89*, 075502.

10.1021/ja067140e CCC: $37.00

air. By comparison, alumino/silicate zeolites and pure silica zeolites can only absorb up to 12 mol % alkali metals and generally require introduction from the vapor phase.[8−12] Alkali metal silica gel materials can be prepared in kilogram quantities by direct combination. Three "stages" of M−SG materials with different reactivities have been prepared.[5] Room-temperature addition to the SG of *liquid* alloys of Na and K form homogeneous loose, black powders (stage 0, denoted M−SG-0). These powders must be handled in an inert atmosphere to avoid ignition. When heated to 150 °C with continual agitation, M−SG-0 forms a loose, black, stage I powder (M−SG-I) that is unreactive or only slowly reactive with dry air. Sodium, being solid at room temperature, does not form stage 0, but molten sodium at 160 °C is absorbed by SG to form the stage I powder (Na−SG-I) When Na−SG-I is slowly heated to 400 °C, a second process occurs. This stage II material (Na−SG-II) is completely stable in dry air and reacts only slowly with normal laboratory air. Although, as is the case for all M−SG materials, it reacts quantitatively with water (based on the total sodium used) to form hydrogen, it does not form radical anions with biphenyl, as occurs with all other M−SG samples.

Determining the structure of M−SG is not straightforward because the materials are not crystalline and involve species intercalated inside an amorphous silica host. Traditional crystallographic methods cannot be used in this case because the intercalants are not periodically arranged. Alternatively, PDF technique has been widely used to study liquids and glasses,[13] and has been applied successfully to study nanostructured materials.[7,14] The PDF gives the probability of finding pairs of atoms separated by a distance r and is obtained by a sine Fourier transformation of the reciprocal space total scattering structure function $S(Q)$. The advantage of using this technique over the traditional Bragg diffraction analysis is that it considers all components of the diffraction intensities. This means that both Bragg and diffuse scattering contributions are considered, which is imperative when information about poorly crystalline materials is required. Because the PDF produces quantitative information about materials that scatter diffusely, it was employed here to assess the nature of the M−SG materials.

^{23}Na MAS NMR spectra provide a direct measure of the relative amounts of neutral sodium and sodium cations that are formed when Na or Na−K alloys are added to silica gel. The chemical shifts of Na^0 and Na^+ are widely separated because of the large Knight shift[15] of the neutral metal. Additional information was obtained from measurements of differential scanning calorimetry (DSC) and magnetic susceptibility.

Experimental Methods

A number of samples were prepared as previously described[5] for room-temperature X-ray scattering experiments and other measurements: (1) Liquid K_2Na and Na_2K alloys were mixed with silica gel at room temperature to form the stage 0 products with up to 40 wt % metal content. Stage I materials were then produced by heating to 150 °C with agitation. (2) Pure sodium was heated to 160 °C with silica gel to produce Na−SG-I samples. (3) Na−SG-I was heated to 400 °C to yield stage II Na−SG.

Samples were loaded into the measurement containers in a helium-filled glove box. DSC measurements used sealed aluminum pans in a Shimadzu model DSC-50 calorimeter. Solid-state ^{23}Na MAS NMR spectra used zirconia rotors in a Varian VXR 400S spectrometer. Chemical shifts are relative to Na^+(aq). Magnetic susceptibility data were obtained with a Quantum Design MPMS2 SQUID Magnetometer. For tests of electrical conductivity, powdered M−SG samples were compressed in a spring-loaded DC powder cell[16] and measured with a digital ohmmeter in a helium-filled glove box at ambient temperatures.

For PDF measurements, samples were packed in flat plate sample holders of 1.0 mm thickness in a helium-filled glove box. Atmospheric oxidation was inhibited by O-ring seals to the Kapton tape windows. X-ray diffraction data were collected by using the rapid acquisition pair distribution function (RA-PDF) technique[17] with an incident X-ray energy of 87.005 keV ($\lambda = 0.142479$ Å) at the 6-IDD beam line at the Advanced Photon Source (APS), Argonne National Laboratory. This procedure facilitates the collection of data in greatly reduced time. Instead of the average 8 h required to collect data with conventional X-ray measurement protocols, the RA-PDF procedure allows a data set to be collected in as little as 3 min.[17] A two-dimensional circular image plate camera (Mar345) 345 mm in diameter was mounted orthogonal to the beam with a sample-to-detector beam path of 204 mm. In order to avoid saturation of the detector, each measurement was carried out with multiple exposure durations, ranging from 100 to 1000 s, depending on the sample. By using *Fit2D*[18] the raw data sets were averaged to improve the statistical accuracy and reduce any systematic error in the experimental setup, normalized with respect to the monitor counts, and then integrated to produce one-dimensional X-ray diffraction data. Data from an empty sample holder and the scattering environment were collected for background subtractions.[7] The total scattering function, $S(Q)$, defined as:

$$S(Q) = \frac{I^{\mathrm{coh}}(Q) - \sum c_i |f_i(Q)|^2}{|\sum c_i f_i(Q)|^2} + 1 \qquad (1)$$

was determined for each sample. Here I^{coh} is the measured coherent scattering intensity, c_i and $f_i(Q)$ are the atomic concentration and X-ray scattering factor, respectively, for atomic species i.[7,19] The corresponding atomic PDF, $G(r)$, was then calculated by Fourier transformation of the reduced structure function, $F(Q) = Q[S(Q) - 1]$, as follows:

$$G(r) = \left(\frac{2}{\pi}\right)\int_{Q_{\min}}^{Q_{\max}} Q[S(Q) - 1] \sin(Qr)\, \mathrm{d}Q \qquad (2)$$

Here, Q is the magnitude of the wave vector, $Q = (4\pi \sin\theta)/\lambda$, where 2θ is the angle between the incoming and outgoing radiation and λ is the wavelength of the X-ray radiation. The reduced structure functions, $F(Q)$, were truncated at a $Q_{\max}$ of 20 Å^{-1} before the PDF was calculated. In order to reduce the effects of noise in the high-Q region and to reduce the effects of termination in the Fourier transform, the $F(Q)$'s for Na_2K−SG-I and Na−SG-I were multiplied by the Lorch function,[20]

$$M(Q) = \frac{\sin(Q\pi)/Q_{\max}}{Q\pi/Q_{\max}} \qquad (3)$$

(11) Rabo, J. A.; Angell, P. H.; Kasai, P. H.; Schomaker, V. *Discuss. Faraday Soc.* **1966**, *41*, 328−349.
(12) Srdanov, V. I.; Stucky, G. D.; Lippma, E.; Engelhardt, G. *Phys. Rev. Lett.* **1998**, *80*, 2449−2452.
(13) Wright, A. *Glass Phys. Chem.* **1998**, *24*, 148−179.
(14) Billinge, S. J. L.; Kanatzidis, M. G. *Chem. Commun.* **2004**, 749−760.
(15) Knight, W. D. *Phys. Rev.* **1944**, *76*, 1259−1260.
(16) Moeggenborg, K. J.; Papaioannou, J.; Dye, J. L. *Chem. Mater.* **1991**, *3*, 514−520.
(17) Chupas, P. J.; Qiu, X. Y.; Hanson, J. C.; Lee, P. L.; Grey, C. P.; Billinge, S. J. L. *J. Appl. Crystallogr.* **2003**, *36*, 1342−1347.
(18) Hammersley, A. P.; Svensson, S. O.; Hanfland, M.; Fitch, A. N.; Hausermann, D. *High Pressure Res.* **1996**, *14*, 235−248.
(19) Warren, B. E. *X-ray Diffraction*; Dover: New York, 1990; pp 369−371.
(20) Susman, S.; Volin, K. J.; Montague, D. G.; Price, D. L. *Phys. Rev. B* **1991**, *43*, 11076−11081.

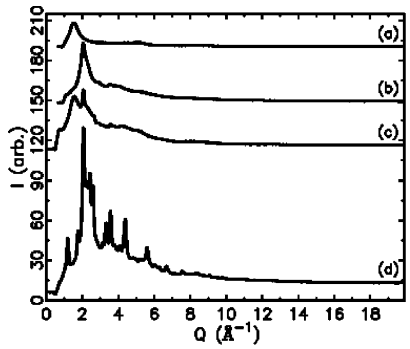

Figure 1. Experimental powder diffraction patterns for (a) pure silica gel, (b) $Na_2K-SG-I$, (c) Na−SG-I, and (d) Na−SG-II. The data were scaled to facilitate easier visual comparison.

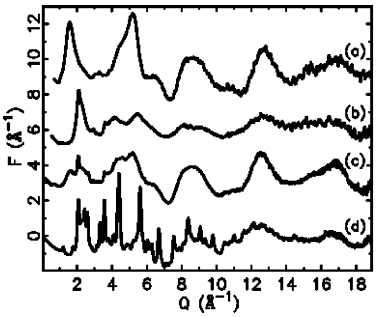

Figure 2. Experimental reduced structure functions for (a) pure silica gel, (b) $Na_2K-SG-I$, (c) Na−SG-I, (d) Na−SG-II.

Conversion of the XRD data to the scattering functions and PDFs was performed using the program *PDFgetX2*.[21] Structure models were fit to the experimental PDF and the parameters refined to obtain the best agreement to the data using *PDFFIT*.[22]

Results and Discussion

Previous work[5] described the preparation and some properties of the three stages of M−SG materials. Stage 0 samples, formed by slowly adding liquid Na−K alloys (with stirring) to silica gel at room temperature, contain small metal clusters in the pores, as determined by the reduced melting temperatures seen in the DSC.[5,23] Stage I samples show no melting endotherm, which was initially taken as evidence for the absence of metal in the silica gel pores of M−SG-I. As shown in the present work, however, a substantial fraction of the encapsulated materials is present as the alkali metal or alloy.

Pair Distribution Functions. Representative X-ray powder diffraction patterns are shown in Figure 1. The resulting structure functions and PDFs are shown in Figures 2 and 3.

It can be seen from Figure 1 that the X-ray diffraction patterns of $Na_2K-SG-I$ and Na−SG-I, (b and c, respectively, of Figure 1) are diffuse in nature and similar in appearance to the diffraction pattern of the pure silica gel (Figure 1a). Na−SG-II (Figure 1d) exhibits a limited number of broad Bragg peaks, which suggests that the reaction products in this material are nanostructured, although there is still a large diffuse component.

Comparison among the data in Figures 1, 2, and 3 illustrates why the PDF approach yields quantitative local structural

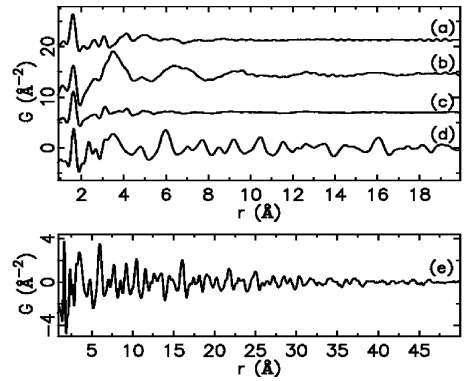

Figure 3. Experimental PDFs, scaled with respect to the Si−O peak amplitude, for (a) pure silica gel, (b) $Na_2K-SG-I$, (c) Na−SG-I, (d) Na−SG-II, (e) Na−SG-II on a different length scale.

information in nanostructured materials. First, the data-reduction step to obtain $F(Q)$ results in an amplification of the important diffuse signal at high Q. In the reduced structure functions (Figure 2) all diffraction features, including those at higher wave vectors, appear equally strong and are therefore similarly important in the structure determination. These features are transferred into the real-space PDF which contains far more directly measurable features than the original XRD patterns. The resulting real-space PDFs are often sharp, well-defined functions.[24] Hence, the enhanced sensitivity to the local atomic ordering in the PDF makes it well suited for the structure determination of materials with limited structural coherence. Once the PDF is obtained, an approach similar to Rietveld analysis[25] can be followed.[26] The effectiveness of this method of solving the structures of disordered materials has been demonstrated previously.[10,14,25]

The features of the reduced structure functions (Figure 2) for $Na_2K-SG-I$ and Na−SG-I are broad, synonymous with the disordered nature of these materials. This disorder is also reflected in the PDFs (Figure 3) which exhibit a rapid falloff in the structural features with increasing r. When compared to pure silica gel, the general features of the reduced structure functions and PDFs of the $Na_2K-SG-I$ and Na−SG-I are similar but still show some differences. In particular, there are broad oscillations present in the PDFs of $Na_2K-SG-I$ and Na−SG-I that extend up to 15 Å and are absent for the pure silica gel. From the similarity in the data it is concluded that $Na_2K-SG-I$ and Na−SG-I retain most of the features of the pure silica structure with the existence of some inclusions indicated by the broad oscillations on the nanometer scale. By neglecting the silica host, we attempted to refine various structures to the nanoscale oscillations at larger r values. Initial trials assumed the alkali metal was present predominantly in metallic clusters.

In $Na_2K-SG-I$, we attempted to fit the ripples at $r > 8$ Å with the ordered Na_2K structure model. Na_2K has a hexagonal structure with space group $P6_3/mmc$ and lattice parameters[27] $a = b = 7.5$ Å and $c = 12.29$ Å. The refinement was not successful as shown in Figure 4a.

(21) Qiu, X.; Thompson, J. W.; Billinge, S. J. L. *J. Appl. Crystallogr.* **2004**, *37*, 678.
(22) Proffen, T.; Billinge, S. J. L. *J. Appl. Crystallogr.* **1999**, *32*, 572−575.
(23) Unruh, K. M.; Huber, T. E.; Huber, C. A. *Phys. Rev. B* **1993**, *48*, 9021−9027.
(24) Peterson, P. F.; Proffen, T.; Jeong, I. K.; Billinge, S. J. L.; Choi, K. S.; Kanatzidis, M. G.; Radaelli, P. G. *Phys. Rev. B* **2001**, *63*, 165211.
(25) Rietveld, H. M. *J. Appl. Crystallogr.* **1969**, *2*, 65−71.
(26) Billinge, S. J. L. In *Local Structure from Diffraction*; Billinge, S. J. L., Thorpe, M. F., Eds.; Plenum: New York, 1998; p 137.
(27) Villars, P.; Calvert, L. D. *Pearson's Handbook of Crystallographic Data for Intermetallic Phases*; American Society for Metals: Metals Park, OH, 1985; Vol. 3, p 2612.

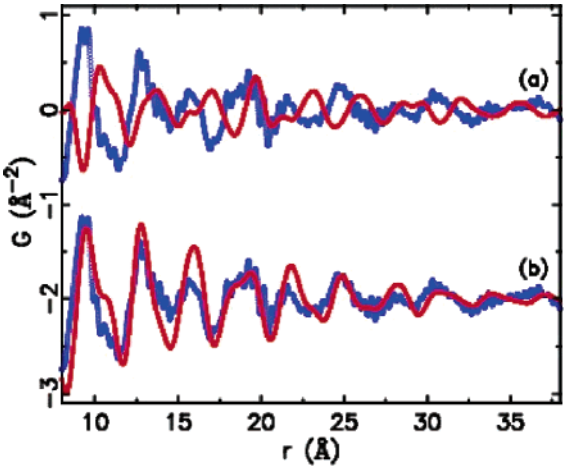

Figure 4. Experimental PDF for Na_2K−SG-I (blue) compared to (red lines): the calculated PDF for (a) the Na_2K hexagonal structure and (b) the Na *bcc* structure.

The ripples were well fit using the simple metallic *bcc* structure, where we assumed that the cluster was a disordered alloy with the same *bcc* structure as that of the end members. We calculated the PDF from the structure of metallic sodium and compared it to the experimental PDF as shown in Figure 4b. Large thermal factors (0.15 Å^2) were needed, indicating a significant amount of structural disorder. The value for U_{iso} is about 10 times higher than one would normally expect for a material at room temperature. This indicates that significant displacive disorder of the atomic positions in the cluster is present in the silica gel. Despite this, ripples consistent with the *bcc* structure are evident in the PDF and extend to at least 37 Å (Figure 4). The *bcc* order therefore extends out to many neighbors to form regular nanoscale metallic clusters with a well-defined lattice spacing of 4.29 Å, albeit with a very large distribution of atomic positions around these average lattice positions. There is a wide distribution of pore sizes in the silica, but the average pore size is 150 Å, much larger than the size of the metallic clusters, which suggests that the structural coherence of the clusters is not completely limited by the confined geometry.

For the case of Na−SG-I, we calculated the PDF from the structure of metallic sodium and compared it to the experimental PDF. The lattice parameter for metallic sodium of 4.2906 Å was used and not refined, but again, large atomic displacement factors (0.1 Å^2) were needed to accommodate the large width of the Na−SG-I $G(r)$ peaks. As is evident in Figure 5, the broad oscillations in the PDF of Na−SG-I that appear in the range of 9−40 Å match very well with peaks from the PDF. This confirms the presence of sodium metal nanoclusters inside the Na−SG-I sample.

The reduced structure function and PDF for Na−SG-II (Figures 2d and 3d) contain more well-defined peaks than the lower-stage materials, indicating more structural order. Figure 3e shows the PDF for Na−SG-II plotted over a wider r range to 50 Å. The PDF signal is seen to taper out at about 48 Å. Since structure is seen in the PDF at this point, the structural coherence clearly extends to 48 Å, indicating clusters of at least that size. The PDF also loses intensity at high r due to finite instrumental resolution. A crystalline silicon standard measured at the same time and under identical experimental conditions showed intensity up to 60 Å, indicating that the observed

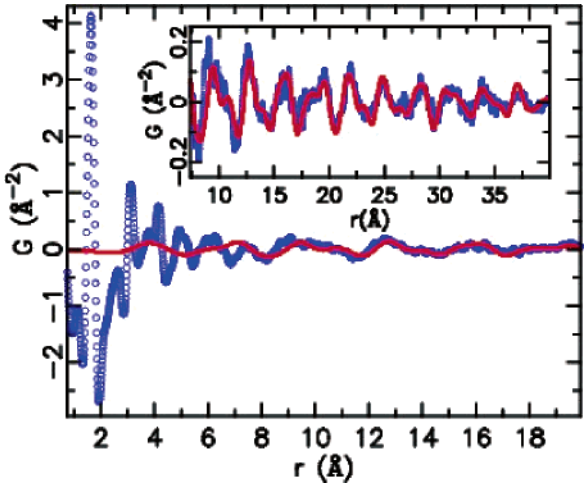

Figure 5. Experimental PDF for Na−SG-I (blue circles) and the calculated PDF for metallic sodium (red lines). (Inset) Same data and best-fit curves in the high r region on an expanded scale. Note that a large silica component has not been subtracted and dominates in the low r region.

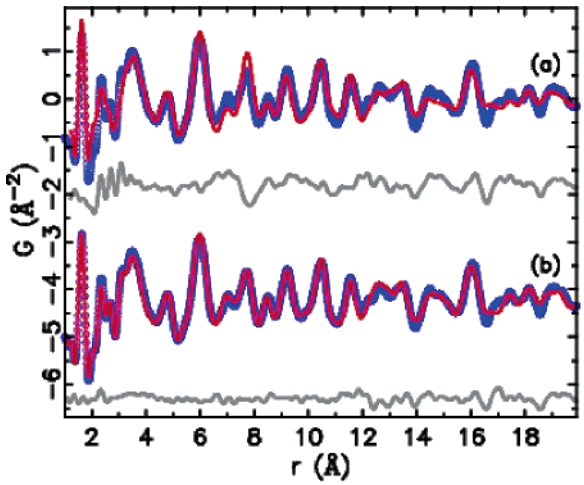

Figure 6. Comparison between experimental (blue points) and calculated (solid red lines) PDFs for the Na−SG-II sample, using (a) a single-phase Na_2SiO_3 model and (b) (offset) a dual-phase model containing Na_2SiO_3 and Na_4Si_4. The residual (gray) plots are shown displaced below each fit.

intensity falloff in the SG-II material is due to sample effects and not instrumental resolution.

When attempting to determine the structure of the stage II material, its proposed stoichiometric formation reaction was considered:

$$5\ Na + 3\ SiO_2 \rightarrow 2\ Na_2SiO_3 + NaSi \qquad (4)$$

Na_2SiO_3 has an orthorhombic structure with lattice parameters $a = 10.43$ Å, $b = 6.02$ Å, and $c = 4.81$ Å.[28] Refinement of this structure to the experimental PDF (Figure 6a) yielded an R_{wp} of 37%. Overall this fit appears satisfactory except for the peaks around 3 Å, where there is an obvious difference between the experimental and the calculated PDF.

To improve the quality of the fit, sodium silicide (Na_4Si_4) was incorporated as the second phase in the refinement. Sodium silicide is known to have the base-centered monoclinic structure, with Na_4Si_4 units and lattice parameters: $a = 12.19$ Å, $b =$

(28) Grund, A.; Pizy, M. M. *Acta Crystallogr.* **1952**, *5*, 837−840.

Table 1. Refined Dual-Phase Structure of the Na−SG-II Material.

Na_2SiO_3				
space group			$Cmc2_1$	
a (Å)			10.43(6)	
b (Å)			6.11(6)	
c (Å)			4.93(6)	
phase fraction	70 mol %			
atom	*x*	*y*	*z*	*U* (Å²)
Na(*8b*)	0.165(6)	0.347(6)	0.00	0.015(2)
Si(*4a*)	0.00	0.118(6)	0.481(6)	0.068(2)
O1(*4a*)	0.000	0.113(6)	0.811(6)	0.041(2)
O2(*8b*)	0.123(6)	0.281(6)	0.500	0.024(2)
Na_4Si_4				
space group			*C*2/*c*	
a (Å)			12.72(6)	
b (Å)			7.25(6)	
c (Å)			10.56(6)	
phase fraction			30 mol %	
atom	*x*	*y*	*z*	*U* (Å²)
Na1(*8f*)	0.292(6)	0.732(6)	0.353(6)	0.009(2)
Na2(*8f*)	0.678(6)	0.046(6)	0.513(6)	0.011(2)
Si1(*8f*)	0.447(6)	0.252(6)	0.323(6)	0.011(2)
Si2(*8f*)	0.624(6)	0.553(6)	0.359(6)	0.031(2)

6.55 Å, $c = 11.18$ Å, and $\beta = 119°$.[29] Inclusion of this structure resulted in a considerable improvement in the refinement fit (Figure 6b) with an R_{wp} of 17%. The structural parameters for the dual-phase model are presented in Table 1. Note that the best-fit phase fractions[30] agree well with the presumed 2:1 reaction stoichiometry.

^{23}Na MAS NMR. Solid-state ^{23}Na MAS NMR spectra provide a good diagnostic for metallic sodium. The paramagnetic Knight shift of metallic sodium is 1040 ppm from that of Na^+-(aq).[15] Thus, peaks in the region of ~1100 ppm provide direct evidence for the presence of Na^0, while those closer to 0 ppm are due to Na^+. Although integrated intensities may not be quantitative for solid-state spectra of quadrupolar nuclei, they provide good estimates of the relative amounts of metal and cation present.

An early indication of the metallic nature of our samples was their effect on sample spinning. Conductive samples are hard to spin in a strong magnetic field because of opposing eddy currents. We found it necessary to dilute many samples with solid boron nitride in order to spin them at 3−4 kHz. This indicates the presence of intergrain conductivity that was confirmed by measurements of the dc conductivity of both stage 0 and stage I samples (vide infra).

The ^{23}Na MAS NMR spectra of stage 0 Na_2K−SG samples with three different average pore sizes showed only the peak of Na^0, with little or no Na^+ peak. This confirms that the metal goes into the pores of silica gel at ambient temperatures without ionization. When converted to stage I by heating (or when Na−SG-I is formed by heating sodium metal with silica gel) some Na^+ is formed, but in large-pore silica gel, a substantial fraction of Na^0 remains. There are several possible sources of Na^+. Reaction of Na with defects, such as SiO^- groups or residual SiOH, would both decrease the amount of reducing material and produce sodium cations. Collection of hydrogen from the reaction with water and comparison with the masses of metal and SG used show that this is a minor effect, amounting to not more than 4 wt % metal. Ionization of Na^0 near or in the walls of the cavities would also produce Na^+, accompanied either by electron donation to the SiO_2 lattice, or formation of an "electron gas" in the void spaces, as occurred with Cs in an all-silica zeolite.[9,10] The driving force for such ionization is the strong interaction of the resulting cations with the oxygens of the silica gel lattice. With large-pore SG, however, a fully loaded sample could have only a fraction of the encapsulated alkali metal atoms close enough to the walls for effective charge-balance. Ionization to form M^+ and an electron gas would be unfavorable if the cations could not be stabilized by the silica lattice. Thus, except for ionized alkali metals in small pores or near the walls, or intercalated into the SG lattice, we anticipate that additional alkali metal would be present as the neutral metal.

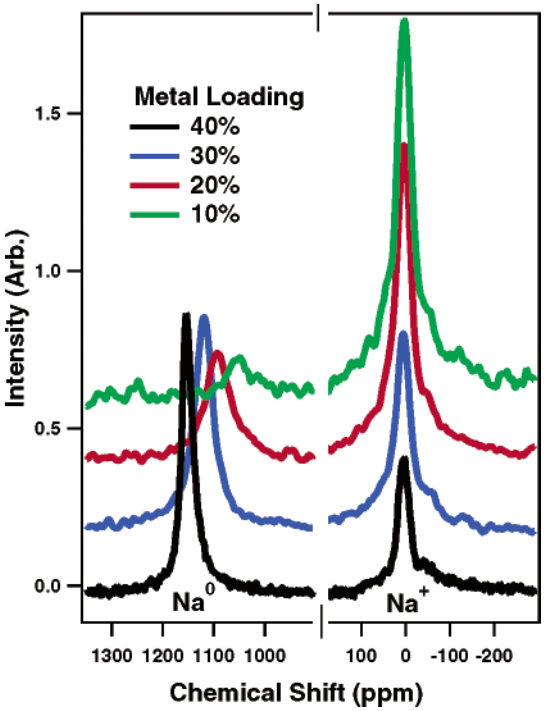

Figure 7. ^{23}Na MAS NMR spectra of Na_2K−SG-I in silica gel with an average pore size of 150 Å at various metal loadings. The weight percent loadings are from the amounts of metal and SG used. The spectra are scaled and displaced for clarity.

Strong support for this picture and for ionization near the walls is provided by the ^{23}Na MAS NMR spectra of Na_2K−SG in silica gel with different pore diameters and different metal loadings. The ratio of Na^0 to Na^+ is strikingly dependent on both the loading and the average pore size of the silica gel used. Figures 7 and 8 show this dependence, and Table 2 gives the approximate metal-to-cation ratios for various preparations, together with chemical shifts and line widths.

In addition to the pronounced effect of loading and pore size on the Na^0/Na^+ ratio, the chemical shift of Na^0 and the line widths of both Na^0 and Na^+ are strongly affected. The chemical shift of Na^+ is constant at 4 ± 1 ppm, but that of Na^0 varies systematically with the Na^0/Na^+ ratio from 1049 to 1154 ppm (Table 2). The line widths of both Na^0 and Na^+ are much broader than is common for either the pure metal or for sodium salts. This could result from quadrupole broadening or a distribution of environments, but the broadening of both lines

(29) Witte, J.; Schnering, H. G. *Z. Anorg. Allg. Chem.* **1964**, *327*, 260−273.
(30) Lin, H.; Božin, E. S.; Billinge, S. J. L.; Quarez, E.; Kanatzidis, M. G. *Phys. Rev. B* **2005**, *72*, 174113.

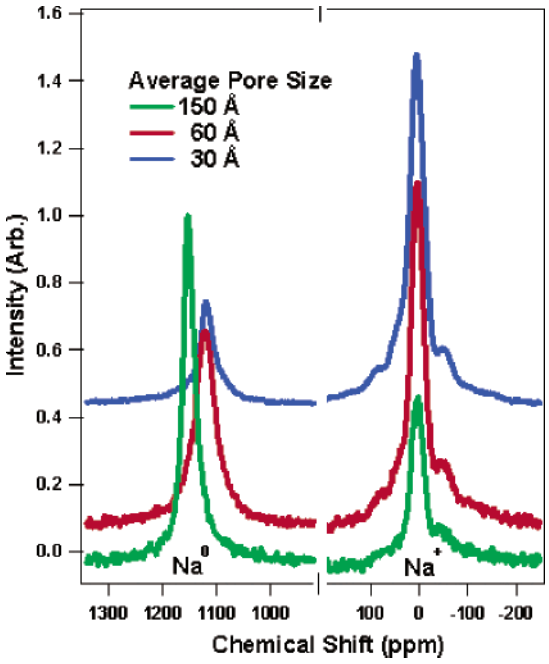

Figure 8. ^{23}Na MAS NMR spectra of Na_2K−SG-I in silica gel as a function of average pore size. Loadings are 40, 35, and 25 wt % metal for 150, 60 and 30 Å SG, respectively. The spectra are scaled and displaced for clarity.

Table 2. ^{23}Na MAS NMR Data for Stage I Metal−Silica Gel Samples

average pore size (Å)	wt % metal	ratio Na^0/Na^+	Na^0 line width (Hz)	Na^+ line width (Hz)	Na^0 chem. shift (ppm)
150	10	0.084	7500	4500	1049
150	20	0.34	5700	6600	1092
150	30	1.02	4400	4200	1119
150	40	1.40	2600	3200	1154
60	35	0.58	4500	2200	1123
30	25	0.25	3400	3900	1120
150[a]	40	1.41	9000	8800	1056

[a] Na−SG sample; others are Na_2K−SG.

and the systematic chemical shift changes of the signal of Na^0 suggest that distributed paramagnetism, a common source of line-broadening, may be responsible. Exchange broadening by interconversion of Na^0 and Na^+ is unlikely, since the line widths are unchanged from −60 °C to +60 °C.

Attempts to obtain more information about the nature of stage I M−SG materials from ^{29}Si MAS NMR studies were unsuccessful because of extremely long T_1 relaxation times, as has been observed for metal−zeolite systems.[9] Data collection for 19 h yielded a signal-to-noise ratio of only 4:1. The chemical shift of the single peak observed was at −83 ppm compared with −118 ppm for calcined silica gel.

As shown in Figure 9, conversion of stage I Na−SG to stage II by heating to 400 °C yields a complex pattern that includes two peaks of Na^+ in the region found previously[31] for Na_4Si_4. The sodium silicate to sodium silicide ratio (5.5), obtained by deconvolution, is close to that expected (4.5) on the basis of the reaction stoichiometry and defect Na^+. There is no peak in the chemical shift range of Na^0. Thus, the ^{23}Na MAS NMR results are consistent with the conclusion from the PDF studies

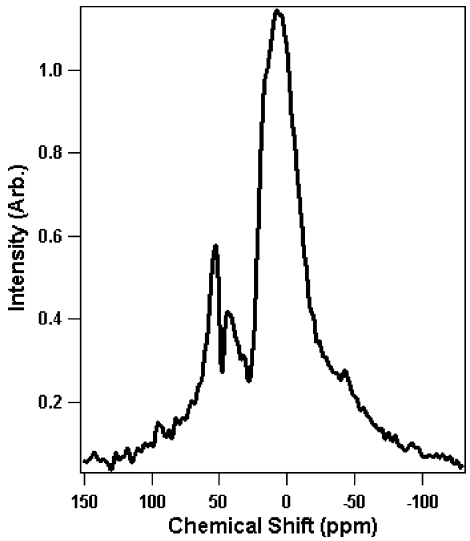

Figure 9. Ambient temperature ^{23}Na MAS NMR spectra of Na−SG-II with average pore size of 150 Å. The two peaks on the left are attributed to Na_4Si_4, while that on the right is from the product sodium silicate and initial Na^+ formed by reaction of Na with defects. This sample has no peak at the chemical shift of Na^0.

that Na^0 reacts completely with SiO_2 to form Na_4Si_4 and Na_2SiO_3. Attempts were made to confirm this with ^{29}Si MAS NMR studies, but the expected peak[31] at −364 ppm from Si_4^{4-} was not observed. Only silicate (or silica) peaks around −100 ppm were observed above the noise. As was the case with Na−SG-I, the extremely long ^{29}Si relaxation time made it difficult to achieve good spectra.

Other Measurements. DSC measurements, described earlier,[5] show that the conversion of stage 0 M−SG to stage I is slow and exothermic, merging with the exothermic formation of stage II material above about 300 °C. The disappearance of the endotherm of melting upon formation of stage I materials has been verified by many experiments with Na−SG, Na_2K−SG, and K_2Na−SG. Although these samples contain alkali metals in the pores, they do not undergo conventional melting transitions. The observation of melting for stage 0 samples shows that mere confinement of metals in the pores does not eliminate the enthalpy of melting. We have no current explanation for the absence of the melting endotherm when stage 0 M−SG is converted to stage I.

The magnetic susceptibilities of calcined silica gel, Na−SG-I, and K_2Na−SG-I (150 Å average pore size) were measured from 5 to 300 K and fit by the Curie−Weiss equation, including a temperature-independent term. The silica gel sample had the most pronounced "Curie Tail" with a paramagnetic content of 0.33 mol %, based on SiO_2. Na−SG yielded 0.027 mol % and K_2Na−SG had 0.066 mol %, based on the moles of metal present. The temperature-independent contribution to the molar susceptibilities, after correction for the diamagnetism of the SG (obtained by an exponential fit of the data above 100 K), was $+14 \times 10^{-6}$ mol^{-1} for Na−SG-I and $+24 \times 10^{-6}$ for K_2Na−SG-I. The molar susceptibility of sodium metal is 15.6×10^{-6} mol^{-1}, while that of potassium is 21.5×10^{-6} mol^{-1}.[32] Thus, the susceptibility data are compatible with the presence of metal in the pores. The small paramagnetism shows that most of the electrons formed by ionization of the metal near or in the SG

(31) He, J.; Klug, D. D.; Uehara, K.; Preston, K. F.; Ratcliffe, C. I.; Tse, J. S. *J. Phys. Chem. B* **2001**, *105*, 3475−3485.

(32) Selwood, P. W. *Magnetochemistry*; Interscience: New York, 1943; p 187.

walls are spin-paired, as was the case with cesium in an all-silica zeolite.[9]

Semiquantitative measurements of the DC electrical resistance of various M−SG samples showed that samples with high Na^0/Na^+ ratios are very conducting, while those that show little or no Na^0 NMR peak are insulating. For example, for samples in SG with 150 Å pore size, the resistance of stage 0 Na_2K−SG (40 wt %) was $<3\ \Omega$, while those of stage I at this concentration as well as at the 25 wt % level were each $<200\ \Omega$. In contrast, the resistances of stage I samples of Na_2K−SG-I at the 20 wt % level and of Na−SG-I (25 wt %) in SG with average pore size 30 Å were each $>2 \times 10^7\ \Omega$. The blank resistance of the lead wires and the empty cell was 1.2 Ω. These results, while not quantitative, indicate that interparticle conductivity occurs by formation of conducting paths between the metal-containing pores, and that samples are insulating when complete or nearly complete ionization of the metal occurs.

Conclusions

A plausible picture that emerges from all of the data for stages 0 and I alkali metal−silica gel materials is that the liquid alloys go into the void spaces at room temperature as neutral metals, without significant ionization. DSC scans of stage 0 powders show the expected low-temperature melting endotherms, the ^{23}-Na MAS NMR spectra show only Na^0, and the electrical conductivity is very high. Heating the stage 0 materials (or Na with SG) results in ionization of some of the alkali metal to produce M^+ at or in the silica gel walls. The cations are stabilized by interaction with the electronegative oxygens of the silica gel, but the nature of the released electrons is open to question. Since the reducing ability (amount of hydrogen formed by reaction with water) is unchanged from that of stage 0, the electrons released by ionization of the included metal are still available for chemical reduction. Indeed, the reduction potential is essentially the same as that of alkali metals. Samples whose Na NMR spectra show only Na^+ and the absence of Na^0 are still able to reduce biphenyl to the radical anion. Most of the released electrons are spin-paired, as is the case with zeolite-based "inorganic electrides".[8,9] An intriguing possibility is the formation of a "skin" of electrons on the surface of the pores, similar to the trapping of electrons in the cavities of organic electrides.[33,34] Organic electrides that have large channels between the cavities show extensive electron spin-pairing. An alternative fate of the electrons is attachment to the SiO_2 lattice, perhaps to form localized "lone pairs" by expansion of the coordination number of Si from four to five,[35,36] or by occupation of the conduction band of the silica gel.

When all of the available sites for M^+ are occupied, additional metal remains in the pores as the neutral metal. The broad NMR lines (temperature independent) and the variation of the line width and chemical shift of the Na^0 NMR peak with loading and pore size indicate that the neutral metal species is influenced by its location relative to the "ionic shell".

Silica gels loaded with alkali metals produce hydrogen when water is added. Stage I samples retain the reducing ability, but not the pyrophoric character of the parent metals, and are thus useful in synthesis. The structures of these materials and the chemical nature of the intercalated species were previously not well defined and could not be determined by traditional crystallographic techniques due to the diffuse nature of their X-ray diffraction patterns. Here we have determined the structures of these materials by using the atomic PDF local structure probe, which considers equally all components of the scattering signal. Comparison of the experimental PDFs with that of pure silica gel indicates that amorphous silica is present in Na_2K−SG-I and Na−SG-I with additional features coming from the intercalants. Broad oscillations in the PDF show that alkali metal nanocrystalline aggregates are present. The structure of the Na−SG-II sample was determined and indicates that Na−SG-II is a dual-phase sample consisting of Na_4Si_4 and Na_2SiO_3, in accordance with the proposed chemical reaction between Na and SiO_2.

Acknowledgment. We acknowledge help in collecting data from Kermit Johnson, Didier Wermeille, Doug Robinson, Pavol Juhas, Ahmad Masadeh, Moneeb Shatnawi, HyunJeong Kim and He Lin. This work was supported in part by the National Science Foundation (NSF)/CHE-0211029/, and in part by SiGNa Chemistry, LLC. The Camille and Henry Dreyfus Foundation provided partial support of K.D.C. PDF data were collected at the 6IDD beam line in the Midwest Universities Collaborative Access Team (MUCAT) sector at the Advanced Photon Source (APS). Use of the APS is supported by the U.S. DOE, Office of Science, Office of Basic Energy Sciences, under Contract No. W-31-109-Eng-38. The MUCAT sector at the APS is supported by the U.S. DOE, Office of Science, Office of Basic Energy Sciences, through the Ames Laboratory under Contract No. W-7405-Eng-82.

JA067140E

(33) Dye, J. L.; Wagner, M. J.; Overney, G.; Huang, R. H.; Nagy, T. F.; Tomanek, D. *J. Am. Chem. Soc.* **1996**, *118*, 7329−7336.
(34) Dye, J. L. *Inorg. Chem.* **1997**, *36*, 3816−3826.
(35) Barrett, P. A.; Camblor, M. A.; Corma, A.; Jones, R. H.; Villaescusa, L. A. *J. Phys. Chem. B* **1998**, *102*, 4147−4155.
(36) Blohowiak, K. Y.; Treadwell, D. R.; Mueller, B. L.; Hoppe, M. L.; Jouppi, S.; Kansal, P.; Chew, K. W.; Scotto, C. L. S.; Babonneau, F.; Kampf, J.; Laine, R. M. *Chem. Mater.* **1994**, *6*, 2177−2192.